CHAPTER 1

Heterogeneous Catalysis: A Sustainable Future

1.1 Heterogeneous catalysis

The term "Catalyst" was first coined by the J. J. Berzelius in 1835 [1]. In particular, the catalyst accelerates the rate of specific reaction without being used itself of undergoing any permanent chemical change and this process is called "Catalysis" [1]. The primary focus of this thesis is "Heterogeneous catalysis" (transition-metals, transition-metal oxides, zeolites, and metal-organic frameworks, etc.), in which catalyst works in a different phase from that of the reactants; typically, the reactants are in the gas phase, whereas the catalyst is a solid material. The chemical reaction efficiency can be improved by using an appropriate catalyst that lowers the barrier for the reaction (activation energy, E_a).

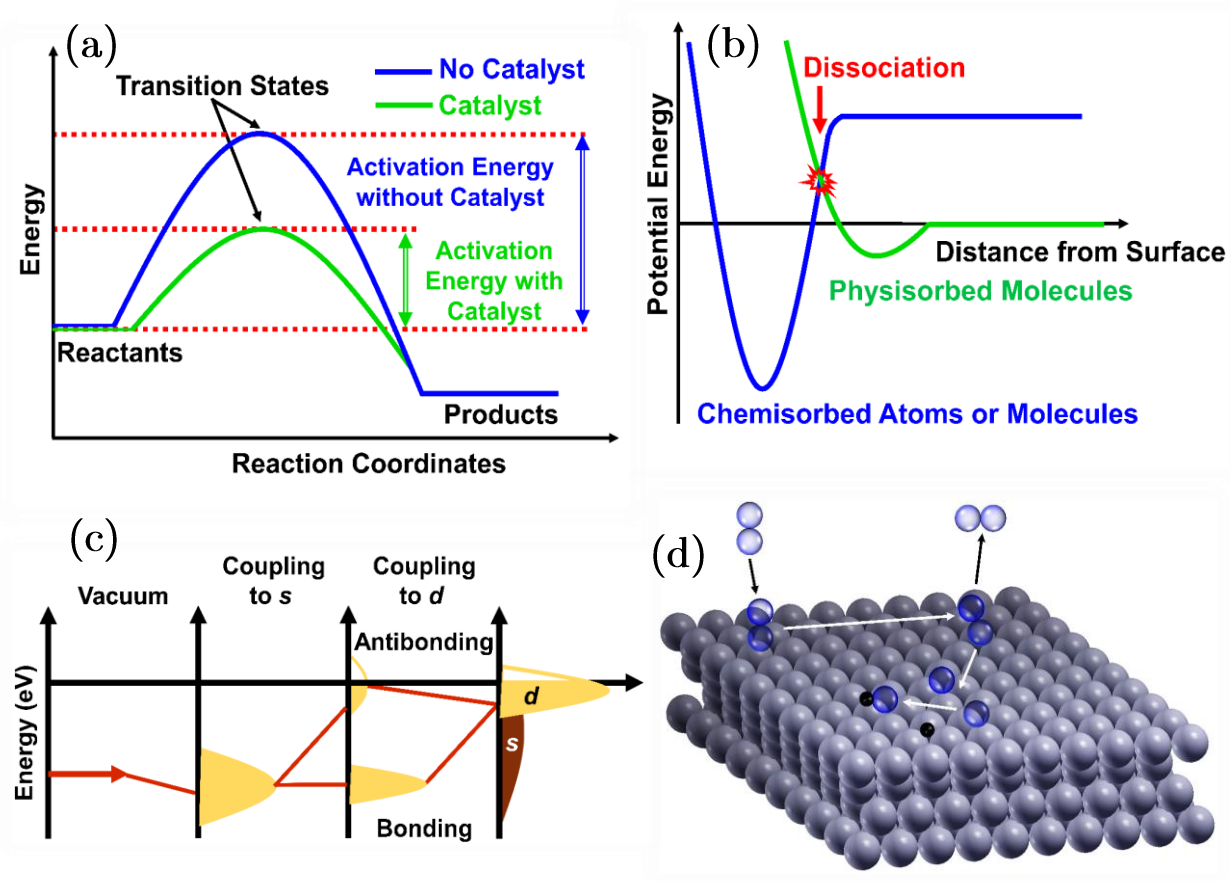

Figure 1.1: (a) Plot of activation energies for an ordinary gas phase reaction (blue) and the same reaction with an appropriate catalyst (green). (b) Energy path for atoms (blue) and molecules (green) approaching a surface. (c) Schematic illustration of the formation of a chemical bond between an adsorbate valence level and the s and d states of a transition metal surface. (d) Illustration of the elementary reaction steps on surfaces.

The activation energy for a gas-phase reaction is compared to that of a catalytic reaction in Figure 1.1(a). The heterogeneous catalysis is a surface phenomenon and hence requires a large surface area to gain a higher yield [2-3]. Therefore, it is necessary to stick an atom or a molecule from the gas phase onto the catalyst surface. This process is called "adsorption" as a whole. The adsorption phenomenon is divided into two classes: (1) when a molecule approaches the catalyst surface, it starts interacting with the surface and forms a bond. If the interaction is long-range caused by dipoles, the molecule is said to be physisorbed over the catalyst surface and the mechanism is known as "Physisorption" and (2) when the molecule goes even closer to the surface, there is a direct interaction between the wave functions of the molecule and the catalyst when the molecule goes even closer to the surface, the molecule is said to be chemisorbed over the catalyst surface and the mechanism is known as "Chemisorption". The relationship between the physisorption and chemisorption reaction as a plot of the potential energy against the distance from a surface for two atoms and one molecule is presented in Figure 1.1(b). The potential energy for the molecule far from the surface is zero as it is unaffected by the attractive van der Waals forces, while it is minimum due to increased electronic repulsion upon approaching the surface. In this reside, the molecule is physisorbed onto a surface and can diffuse over long distances if the temperature is not too low. When the physisorbed molecule collects enough energy to approach the surface at a sufficient distance (close to the surface), depending on internal bond strength, the molecule either dissociates into atoms or chemisorb molecularly [4]. Figure 1.1(c) presents the schematic illustration of bond formation at a transition-metals (TMs) surface. The lower the d states in energy relative to the Fermi level, the antibonding states are more filled and weaker is the adsorption bond [5]. When reactants are adsorbed and perhaps dissociated, they will diffuse and recombine to form new molecules before the product is desorbed into the surrounding gas or liquid phase [3]. These elementary surface reactions are illustrated in Figure 1.1(d).

Catalysis has received enormous interest from the perspectives of both scientific research and industrial applications [6]. To date, heterogeneous catalysts account for ca. 80% of industrial catalytic processes due to their easy recovery and robustness (see Figure 1.2(a)) [7]. The catalyst market alone contributes to approximately 30% of global gross domestic product (GDP) [8].

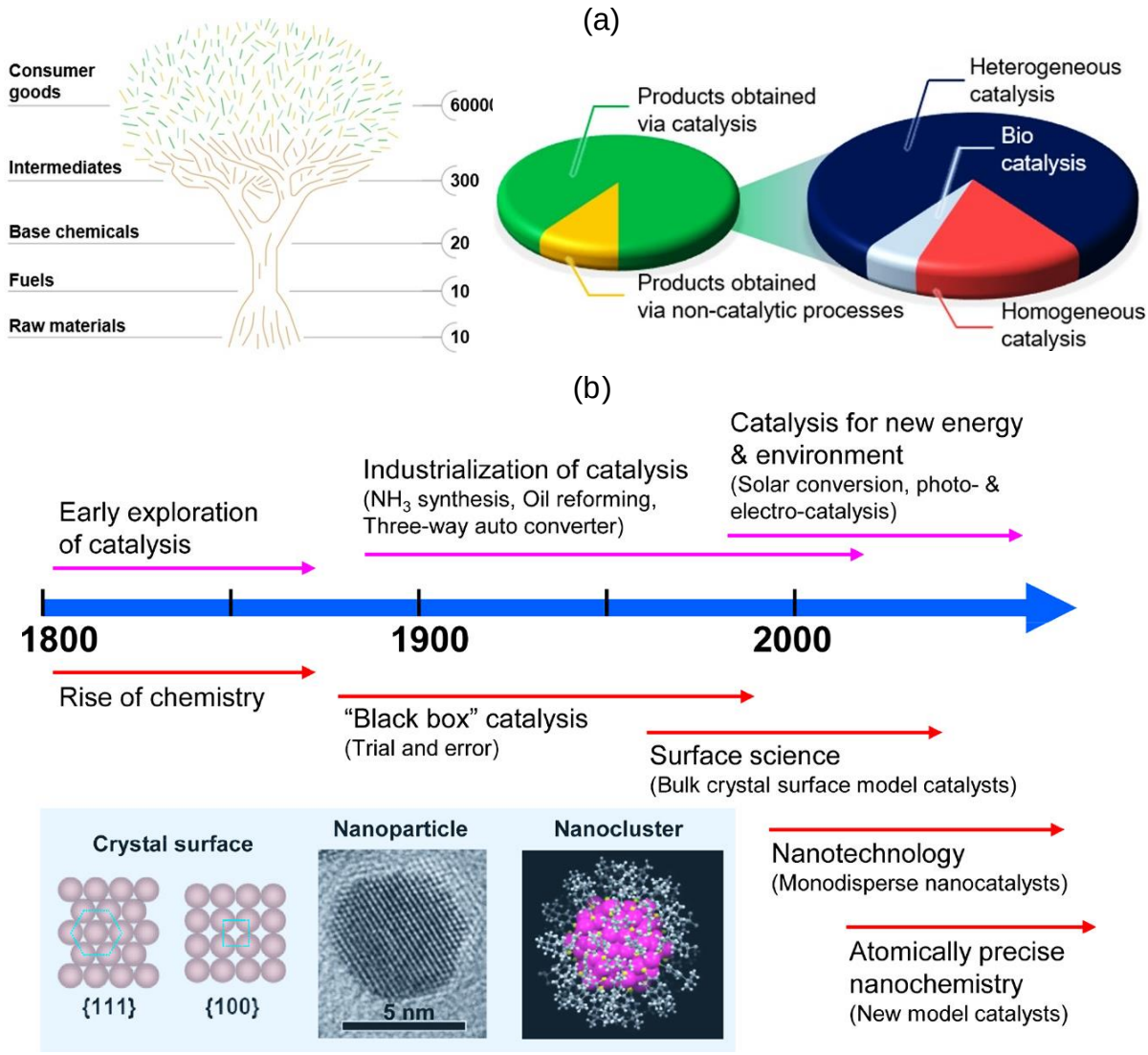

Figure 1.2: (a) Relevance of catalysis for the chemical industry. Over 90% of the world's manufactured consumer goods involve catalysis at one or more stages. Approximately 80% of all catalytic processes require heterogeneous catalysts, 15% homogeneous catalysts, and 5% biocatalysts [7]. (b) The evolution of heterogeneous catalysis from the 19th to the 21st century [2].

The demand for novel catalytic technologies is ever-growing to secure a sustainable future of modern society [9]. Future developments of these technologies are expected to heavily rely on catalysis, in particular, clean energy conversion and environmental protection. A major goal of these developments is to pursue highly selective and efficient catalytic processes under mild conditions. Academically, the catalysis sector has also been promoting the advancement of science and pushing forward the frontiers of human knowledge (see Figure 1.2(b)). About twenty Nobel Prizes have been awarded for research related to "catalysis" [10]. From a practical point of view, heterogeneous catalysis has been emerged significantly in recent years [11-13], largely built on the success in the synthesis of monodisperse metal nanoparticles (NPs) with tight size distributions (5−15%) by wet chemistry.

Particularly for metals and their alloys, significant surface mobility may arise under relatively mild reaction conditions, leading to surface morphological variations [14]. Under these situations, it is tricky to draw structure−activity correlations and gain molecular-level insights. For this reason, it is highly demanding to design novel heterogeneous catalysts with more uniform, spatially separated, and structurally fixed active sites. A new direction is to develop atomically precise nanoclusters (NCs) for catalysis [15]. Compared to conventional NPs whose structures are often vague and non-uniform, NCs have specific geometry in both the core and the surface with atomic precision and are molecularly uniform as well. Hence, the NCs-based catalysts can provide unprecedented opportunities for fundamental catalysis research [16-17]. The catalytic performance of metal NCs and their alloys is often regulated by quantum size effects owing to their reduced dimensions, in contrast to their conventional bulk counterparts. Rational design and improvement of heterogeneous catalysts with high activity and selectivity rely on the fundamental understanding of key parameters (descriptors) that determine the surface-mediated bond activation, formation of reactants, and intermediates [18].

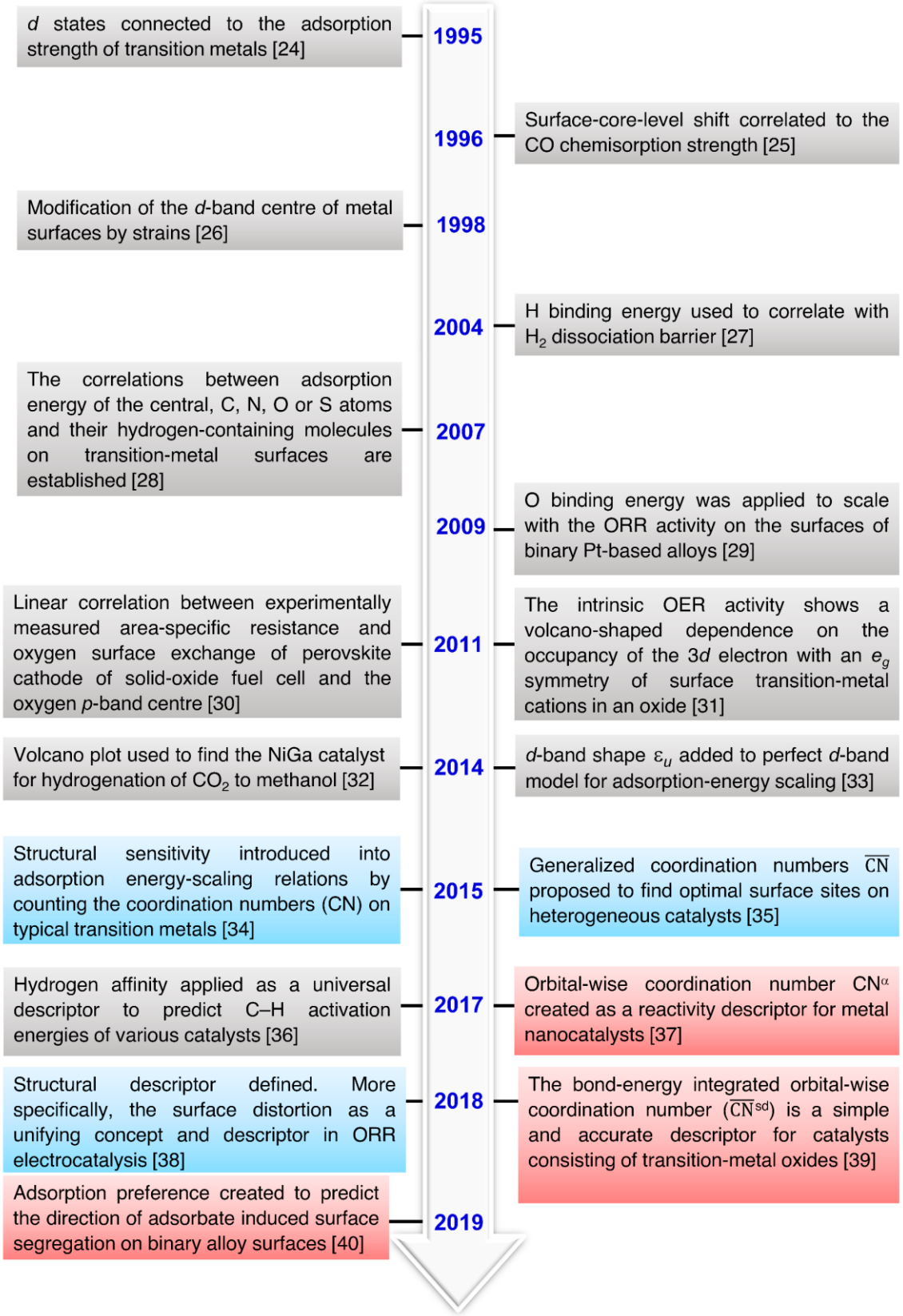

Figure 1.3: A timeline of the development of reactivity descriptors and scaling relationships in heterogeneous catalysis [18]. The grey, blue, and pink boxes represent electronic, structural, and binary descriptors, respectively.

It is the establishment of structure-activity relationship using model and platform chemicals, based on which the sustainable production of a wide spectrum of chemicals and fuels can be developed such as carbon dioxide (CO_2) reduction into C1 and C2 products [19]. These days, theoretical simulation offers a more rational way to design novel catalysts. By employing, density functional theory (DFT) calculations and other theoretical methods, reaction mechanisms at the atomic level can be determined [20-21]. Concurrently, the scaling relationship to construct reactivity descriptors such as the electronic structure of the catalyst, the binding strength of intermediates on the surface, and a range of geometric properties have enhanced our knowledge of the catalytic process and has been intensively investigated [5,22-23]. The timeline on the development of electronic descriptors, structural descriptors, binary descriptors (in which both electronic and structural properties are considered), and elementary universal descriptors is presented in Figure 1.3 which formulate the foundations for the future computational design of catalysts [18,24-40].

1.2 Transition-metal nanoclusters and nanoalloys

There are notable uses of TMs in various technologically vital areas attributed to their excellent catalytic, electronic, and magnetic properties. Enhancement in properties is possible when two or more of these metals are combined [41]. The use of nanoalloys (NAs) has been reported since the 19th century, when Michael Faraday studied optically active Au-Ag nanoparticles [42], however, without a clear understanding of the underlying physics and chemistry [43]. Advancement in methods and characterization techniques made it possible for modern research to utilize the diversities in NAs compositions and chemical ordering such as intermetallic, random, non-random, or phase segregation [41], including size, atomic order, and structure.

Metal NCs and NAs in pure or mixed metallic aggregates of dimensions ranging from 1-100 nm (~10 to 10^6 atoms or molecules within a nanometer size range) are the

subjects of great interest in basic science as well as in advanced technology where they find many applications starting from chemical sensing to heterogeneous catalysis, from magnetic recording to optoelectronic devices owing to their unique properties [44]. NCs can present both crystalline (e.g., face-centered cubic (fcc), octahedra, or TO with large clusters) and non-crystalline (e.g., icosahedra, decahedra, cuboctahedral, and tetrahedral) structures [41,45] (see Figure 1.4). The cluster system could be neutral or ionic and composed of either single or more species, stabilized in certain (physical or chemical) media, for instance, fullerenes, metal clusters, molecular clusters, and ionic clusters [2]. The most remarkable features of clusters are the size-dependent evolution of structure and quantized electronic energy levels, giving rise to an atomic-like character.

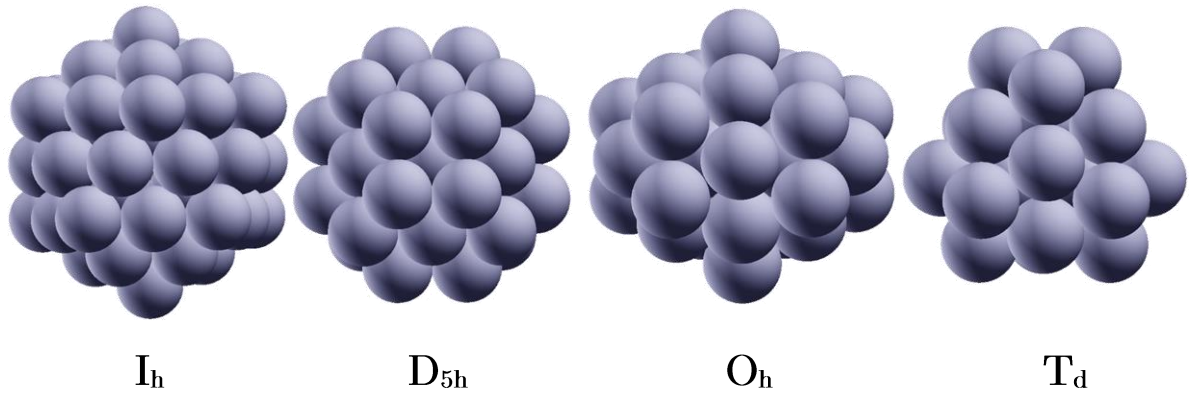

Figure 1.4: Schematic of pure metal clusters. From left to right: icosahedral, decahedral, cuboctahedral, and tetrahedral, with point group symmetries.

These phenomena have been directly associated with the enhancement in the optical and electrical properties of some clusters [44,46]. The spherical jellium model [47] can be used to describe the shell closing behavior of NCs and NAs. Similar, to inert gas atoms, filled shells (shell closing) are relatively stable and give rise to magic sizes that correspond to n = 2, 8, 18, 20, 34, 40, 58, ... number of electrons [48]. Shell closing effects have been identified as the main reason for the occurrence of even-odd effects in the mass spectral abundance, ionization potential, and other properties of clusters [49]. The NCs of group 10 (Ni, Pd, Pt: active group), group 11 (Cu, Ag, Au: less active/inactive group), and their crossover combinations (careful selection of method and alloy

combination) offer unique physical and chemical behavior, with the possibility of fine-tuning size and structures that are of great importance credited to their exceptional physical, optical, electronic, magnetic and especially catalytic properties [2,46]. Upon alloying, activity, selectivity, and stability boost are possible. Another dimension i.e., "chemical ordering" arises in the form of core-shell, subcluster, segregated, mixed, and multiple shells. The adopted chemical arrangement of NAs may be influenced by a complex competition between many factors such as relative strengths of homo- and heteronuclear bonds, relative atomic sizes, surface energies, charge transfer, electronic/magnetic effects, and external (environmental) effects [2,46]. To date, promising results are reported for a wide range of catalytic applications of NAs such as carbon monoxide (CO) oxidation (Ni-Cu [50]), steam reforming of *n*-butane (Ni-Au [51]), NO reduction (Pt-Cu [52]), oxidation and hydrogenation of CO and unsaturated hydrocarbons (Cu-Pd [53], Pt-Au [54]). Much emphasis on structure-activity relationships is made in experimental and theoretical investigations, to fabricate new materials with well-defined and controllable properties. Detailed theoretical studies can extend our understanding of these complicated systems, providing a better understanding of experimental observations and allowing the prediction of chemical and physical properties. The electronic and/or geometric effects and their interplay with structure-activity relationships of NAs found very interesting owing to the possibility of fine-tunning of catalysts that need optimum strength (neither too strong nor too weak) of adsorbate-substrate interactions [55]. Electronically, this is possible via electron transfer by a flow of charge [56] or modifications in the *d-band* center [22-23,33]. The latter is supported by X-Ray Photoelectron Spectroscopy (XPS) and X-ray Absorption Near-Edge Structure (XANES) experiments coupled with theoretical calculations [2]. However, some researchers disagree by stating that the improvement arises from dilution of the metal surface [57]. The geometric effects also contribute to the catalysis process, as changes in size and/or geometry of the cluster lead to alteration of electron bandwidth

and core electrons, as well as the exposed planes and the surface topology [55,58]. Large clusters contain high coordination sites (facets, planes), however, size reduction introduces more activated sites (kinks, edges, corners), which thereby provides a more active catalyst. In NAs, more than one type of metal may occupy active sites, which is required in some reactions. Moreover, intermetallic interactions produce different neighboring atoms and new activated sites (e.g., point defects, interfaces, edges) [41]. Furthermore, electronic, geometric, ligand, and ensemble effects affect the *d-band* center position which is crucial for catalytic activity. However, there is also an economic driving force for NAs research as low-cost (Ni, Cu, and Co) metals can be replaced by expensive noble metals such as palladium, platinum, and ruthenium without reduction in the activity [2].

Catalytic enhancement of Pd- and Cu-based nanocatalysts display significant development for the CO_2 hydrogenation to methanol (CH_3OH), formic acid (HCOOH), and methane (CH_4) [59]. The combination between Pd-Cu is one of the most interesting binary systems of these groups, especially for their immense potential as a catalyst [60]. A detailed discussion of this system will be presented in Chapter 4. Although many theoretical calculations have focussed on the free clusters, it is difficult to get interaction-free clusters. As an alternative, reactive or non-reactive supports have been included. This adds extra complexity when determining the geometric structures and stabilities of the clusters. However, the inclusion of support is very stimulating from a catalysis point of view, as distinct behavior from a variation of support is expected. In the following, we will review some of the important materials as supports.

1.2.1 Supported clusters

Supported metal catalysts are an important group of heterogeneous catalysts, usually comprising of small metal particles dispersed over a porous substrate. The substrate, or in industrial terms, the carrier is expected to meet several requirements such as exposing a high surface area, exhibiting high mechanical and thermal resistance.

Metal oxides meet all criteria required for heterogeneous catalysis, for instance, high thermal and chemical stabilities combined with a well-developed structure and high surface areas (>100 m^2g^{-1}). As discussed in section 1.2, TMs NCs/NAs of group 10 (Ni, Pd, Pt) and group 11 (Cu, Ag, and Au) are of particular interest to this thesis, as they catalyze oxidation, (de)hydrogenation, cyclization, isomerization and other vital reactions [61]. The benefits of having supported TMs NCs/NAs incorporate the following aspects: (1) the catalyst is easily and safely treated compared to the NCs/NAs in the gas phase, (2) the catalysts may be used in a variety of reactors, and if used in a liquid medium they may be recovered by filtration, (3) because NCs/NAs are well-disconnected from each other, they do not grow in size by sintering when heated to high temperature in a reducing atmosphere [62] and (4) the support provides a means of bringing promoters into close contact with the NCs/NAs. Here, it is instructive to illustrate the correlation between exposed (specific) surface area and the size of the NCs/NAs. It is understood that the smaller NCs/NAs will have a larger specific surface area or higher dispersion, which may result in an enrichment of catalytic activity.

This explosive journey of oxide supported TMs NCs/NAs fired up with the Haruta and co-workers' pioneering work [63] on the exceptional catalytic activity of Au NPs of 2 to 5 nm in diameter supported on oxides towards CO oxidation at temperature as low as -76 °C, close to the coldest ambient temperature on this planet (-89.2 °C at Vostok in Antartica). This inspirational work leads to the so-called "Gold- Rush Era" in heterogeneous catalysis [64-66]. To date, there has been no common consensus about the source of such high catalytic activity of nanogold, and it is normally accepted that the catalytic activity of Au depends to a large extent on the size of the Au particles, and other effects were also proposed to be of fundamental importance, for instance, the nature of the substrate, particle/support interface, charge transfer between NPs and support [67]. Goodman et al. [68] commented that the thickness, shape, and oxidation state of Au NPs are responsible for the high catalytic activity based on findings

comprising a bilayer Au model catalyst supported over TiO_X. In the case of oxide support, the reducible (active) oxides e.g., CeO_2, Fe_2O or TiO_2 having a lower ionic character and a small bandgap are superior to nonreducible (inert) oxides such as SiO_2, MgO, or Al_2O_3 that possesses marked ionic character and a wide bandgap, under similar conditions [69-71]. This may be accounted for the fact that the synergistic effect between active oxides and supported metal clusters is comparatively stronger, and the support-mediated oxygen transport, in other words, oxygen is released from the oxidic support which diffuses over the support surface to the edges of the metal particles, where the CO oxidation reaction occurs.

Depending on the catalyst (NCs/NAs) being studied, a support can be chosen based on reaction requirements. For example, the presence of Au-O back-bonding with Al_2O_3 support is attributed to enhanced reactivity in the Au-catalyzed oxidation of CO. An analogous observation is, however, not detected for Au/SiO_2 and Au/TiO_2 catalytic systems, in which Au structures remain unperturbed [72]. Metal-support interactions have a targeted and very specific function in catalytic reactions. In the conversion of CH_3OH to CO_2, the Pt NCs performance order is $Pt/MgO \geq Pt/TiO_2 >> Pt/Al_2O_3$. Combustion in ammonia (NH_3) atmosphere still prefers the MgO support. Analysis of the XPS reveals the metallic state of Pt and strong interaction with the TiO_2 and Al_2O_3 support which give rise to vulnerable catalytic behavior. In contrast, there is no evidence for interaction between Pt and MgO support [73]. One might argue that the improvement of catalysis might be due to support participation. which is not always true as inactive γ-Al_2O_3 are reported to increase the action of Pt catalysts in the hydrolysis of NH_3BH_3. In this reaction, hydrogen release rates are in the order Pt/γ-$Al_2O_3 > Pt/C > Pt/SiO_2$, with a strong influence of particle size [74]. According to previous findings on CO_2 reverse water-gas shift reaction, the catalytic activity decreases in the order of $Ni/CeO_2 > Cu/CeO_2 > Co/CeO_2 > Fe/CeO_2 \approx Mn/CeO_2$. Moreover, Cu/CeO_2, Fe/CeO_2, and Mn/CeO_2 catalysts maintained 100% CO selectivity at the

temperature of 400°C [75]. Currently, the most active catalysts for the hydrogenation of CO and CO_2 to CH_3OH are based around Cu/ZnO catalysts, with $Cu/ZnO/Al_2O_3$ already being commercialized in the production of CH_3OH from CO [76]. Au and Cu supported on various metal oxides have been investigated in the conversion of CO_2 to CH_3OH, with only Au/ZnO exhibiting a comparable activity to that of a standard Cu/ZnO [77]. Therefore, it is very obligatory to understand the surface structural phenomenon, the material dependence of each elementary step, and the overall reaction, and eventually designing catalysts for specific reactions is of great interest and a tremendous challenge to researchers.

1.3 Reaction mechanism for CO oxidation

The oxidation of CO to CO_2 is vital in automotive exhausts and low-temperature fuel cells for environmental and health-friendly emissions.

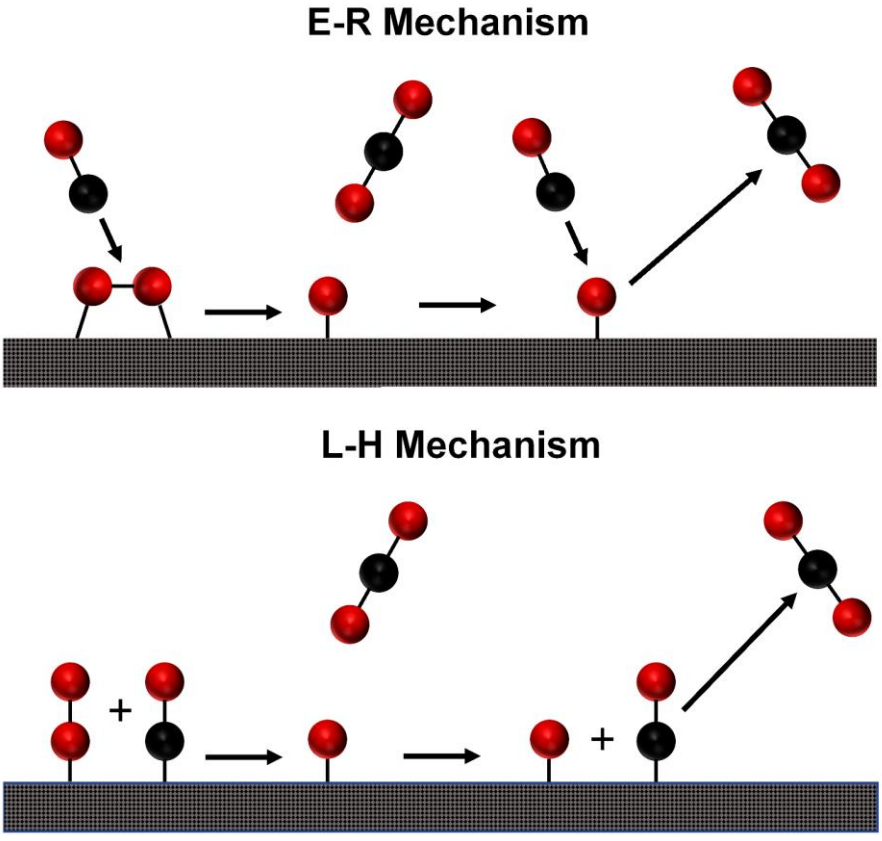

Figure 1.5: The schematic illustration of E-R and L-H mechanism pathway for CO oxidation.

The oxidation of CO on catalyst majorly takes place via the Eley-Rideal (E-R) or the Langmuir-Hinshelwood (L-H) mechanisms. In the E-R mechanism, gas-phase CO molecules directly attack the activated O_2 (with or without dissociation) which is adsorbed on the surface of the catalyst. While, in the L-H mechanism, CO and O_2 (with or without dissociation) molecules are co-adsorbed on the adjacent sites of the catalyst surface state [78]. The schematic representation for both the CO oxidation method is presented in Figure 1.5. These two reactions are divided into two parts: the first half of the reaction is $CO + \frac{1}{2}O_2 \rightarrow CO_2$ and the second half of the reaction is $CO + O \rightarrow CO_2$.

1.4 CO_2 hydrogenation

One exciting area of research is the CO_2 hydrogenation to hydrocarbons (such as CH_3OH, CH_4, and HCOOH), as this not only produces a value-aided chemical fuel but replaces technologies that pump a lot more CO_2 into the atmosphere. The production of CH_3OH and hydrocarbon fuels via CO_2 hydrogenation is regarded as the most viable way of reducing CO_2 emissions in the atmosphere significantly [79]. The CO_2 hydrogenation to hydrocarbons can be seen as a modified Fischer-Tropsch synthesis (FTS) with CO_2 as a reactant instead of CO. Some of the main products of CO_2 hydrogenation are CH_3OH, HCOOH, and hydrocarbon fuels which depend on the type of catalyst and reaction conditions.

CO and water (H_2O) are considered as by-products of the reaction. The CH_3OH is a very desirable reduction product of CO_2 due to its numerous applications [79-81]. The diverse applications of CH_3OH are shown in Figure. 1.6(a) along with projections of future CH_3OH usage in Figure 1.6(b). The global CH_3OH market size was approximated to be USD 38.9 billion in 2018 and is forecasted to rise at a cumulative average growth rate (CAGR) of 9.8% from 2019 to 2026 [80].

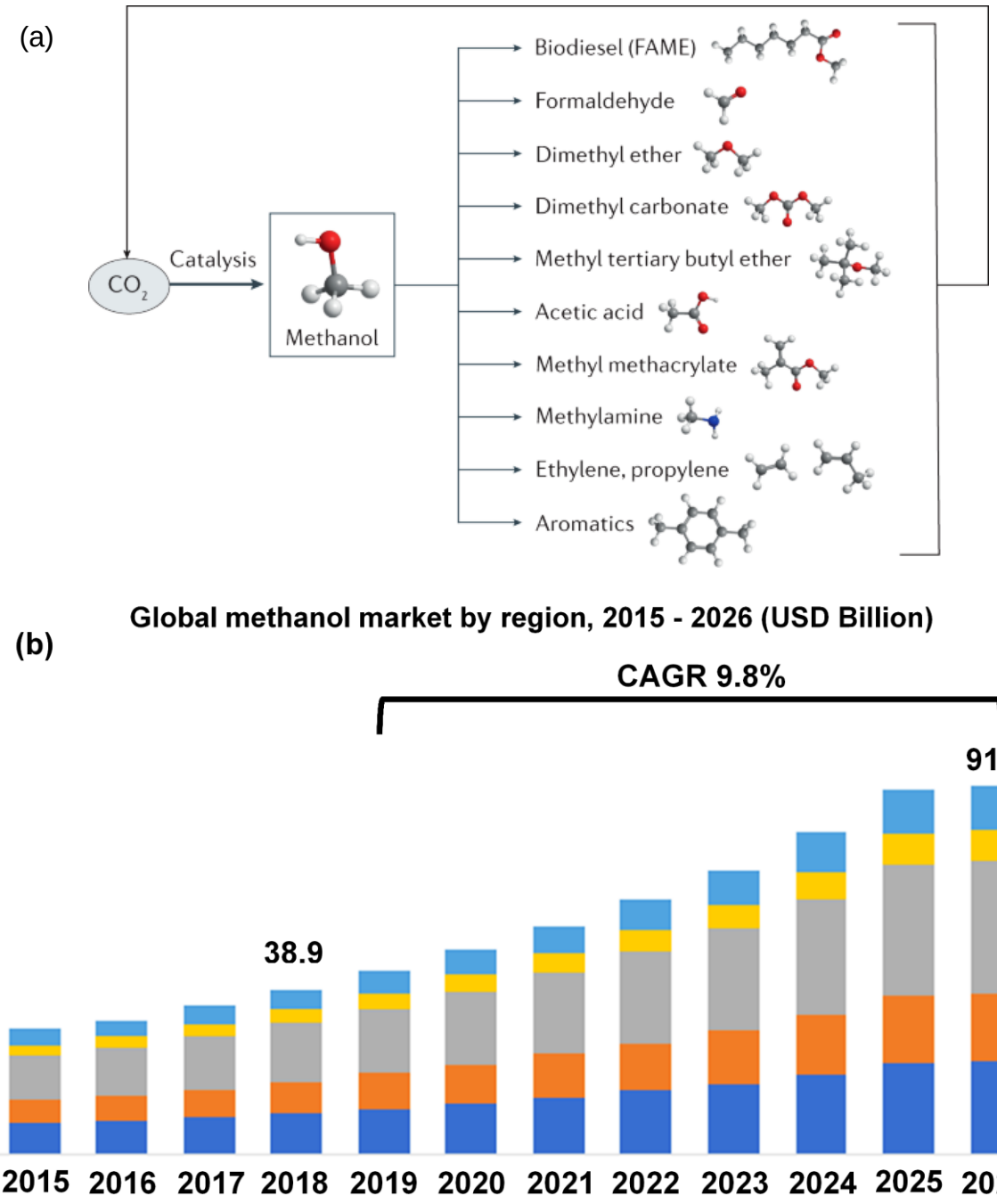

Figure 1.6: (a) Carbon cycle of CH_3OH, a platform molecule for the chemical industry [79]. (b) Trend analysis on global CH_3OH market size and forecast by end-use [80].

However, understanding the complex reaction pathways of CO_2 hydrogenation is very difficult because a large number of intermediates and the rate-limiting step(s) are not well determined. The schematic of complete reaction roadmaps of CO_2 hydrogenation is

presented in Chapter 4. The pathway can be various for different catalysts, and one can construct other similar reaction routes using the same concept [82].

1.5 Thesis motivation and objectives

Free and TM oxides supported catalysts are renowned for their catalytic properties, however, an understanding of their electronic structure is lacking when compared to other material categories [18,45]. Traditional approaches for catalyst design rely on trial-and-error tests because of the complex structures of supported catalysts and the limited in situ characterization techniques. The rational design of efficient and highly active catalysts requires a fundamental understanding of the origin of catalytic activity on account of energetics and interactions that occur at the atomic level over nanostructured materials which is, in general, a hard task via experimental techniques performed at real conditions. In particular, compositions at the atomic level (bond lengths and coordination numbers), the structural fluxionality, modulation in the electronic structure of systems (atom wise orbital contribution in electronic band structure, electronic density of states, electronegativity, and oxidation states of specific atoms), bonding configurations, charge transfer mechanism, vibrational properties and interaction among adsorbent−adsorbate throughout the reaction pathway provide useful insight while studying heterogeneous catalysis. Recent advancements (computer processor), investment (supercomputing facilities), and higher accuracy (theoretical methods) in the density functional theory calculations provide a clear view of the undefined factors that influence the performance of the experimentally synthesized free as well as supported catalysts. The theoretical modeling offers an advanced form of characterization that can be compared with and often complements experiments, but they are also uniquely able to explore high energy intermediates or transition states which can be of fundamental importance in the catalytic pathway but could otherwise be ignored as they escape experimental characterization. In this context, a computational

study is often the only practical and potentially accurate source of structural information, especially when insight into dynamic processes such as catalysis is sought.

The present thesis work aims to understand and predict the catalytic activity of free and oxide-supported NCs and NAs by employing first-principles calculations. Further, the work also aims to develop and design novel strategies and practical methodologies to control catalytic performance towards important chemical reactions (for example, CO oxidation and CO_2 hydrogenation) of the catalysts, with the evaluation of reaction barriers and catalytic mechanisms. The specific objectives of the research work presented were:

a. Determination of equilibrium ground state (energetic) and geometrical structures or active surfaces (atomic configurations) of group 10 (Ni, Pd, Pt), group 11 (Cu, Ag, and Au) NCs, and NAs with various sizes and deposited over various oxide supports.
b. The analysis of formation enthalpy to find the diameter (shape) dependent thermodynamically most stable structure.
c. To compute electronic band structure, electronic density of states, and charge density contour.
d. To examine the effect of various kinds of defects such as vacancies and impurity atoms, and the interactions between them. These investigations will be important as defects are known to have a significant effect on the bonding and electronic properties of heterogeneous ultra nanocatalysts.
e. To study the vibrational and allied properties using first-principles calculation.
f. To examine the magnetic moments using full-potential, spin-polarized DFT calculations.
g. Study the performance of clusters with adsorbed ligands in the form of reactants, products, and intermediates during oxidation and reduction reactions.

1.6 Thesis organization

The thesis consists of six chapters. **Chapter 2** briefly introduces the theoretical framework used in this study. Results of the theoretical calculations will be described in **Chapters 3–5** and finally, the conclusions of the thesis work will be given in **Chapter 6**. In every chapter, a brief introduction of the topic will be outlined, followed by the details of the computational studies, discussion of the results, and conclusions.

Chapter 2 gives a brief introduction to the electronic structure calculations Density Functional Theory (DFT) along with Grimme's dispersion corrections (D2 and quite recently improved D3) and the research methodology for structural optimization in detail. Additionally, the methodologies to determine the reaction barriers during catalytic reactions are also briefly discussed.

Chapter 3 presents the first-principles calculations based on spin-polarized DFT to unveil the role of the Cu atom in the degrading CO poisoning mechanism over Ni_nCu clusters [50]. Initially, this chapter addresses the systematic investigation of structural, magnetic, and electronic properties of Ni_{n+1} and Ni_nCu clusters ($1 \leq n \leq 12$) along with the X-ray absorption near-edge structure (XANES) spectra of Ni K-edge to extract the information of the oxidation states and coordination environment of metal sites of clusters. In addition, the spin-dependent quantum chemical descriptors for Ni_{n+1} and Ni_nCu clusters are also presented in detail. The CO adsorption over considered clusters with the two forms of dispersion corrections i.e., D2 and D3, electronic reactivity descriptors such as *d-band* center, *d-band* width, and fractional filling of *d-band* and effective Löwdin charge are examined and analyzed. The CO oxidation reaction pathway within the Langmuir-Hinshelwood (L-H) mechanism over representative cluster systems is also presented and discussed in detail. This chapter provides a valuable strategy for the rational design of catalyst in essence to CO oxidation with no Ni-poisoning [50]. The findings reported in this chapter have appeared in the following publication:

- B. A. Baraiya, H. Tanna, V. Mankad, and P. K. Jha, Dressing of Cu Atom over Nickel Cluster Stimulating the Poisoning-Free CO Oxidation: An Ab Initio Study, The Journal of Physical Chemistry A, DOI: 10.1021/acs.jpca.1c02354.

Chapter 4 addresses the structural stability, electronic properties, and effect of metal-metal interaction on Raman spectra of icosahedral (I_h) Pd_mCu_n (m + n = 13) clusters using first-principles calculations based on density functional theory [83]. This chapter also encompasses the investigation of CO_2 adsorption over Pd_mCu_n (m + n = 13) clusters and CO_2 hydrogenation over specific clusters for the production of value-added chemicals and fuels. The systematic doping of Cu and its effect on the parent cluster and heterogeneous catalytic activity are also discussed in detail. The results presented in this chapter have appeared in the following publications:

- Bhumi A. Baraiya, Venu Mankad, Prafulla K. Jha, Uncovering the structural, electronic, and vibrational properties of atomically precise Pd_mCu_n clusters and their interaction with CO_2 molecule, Spectrochimica Acta Part A: Molecular and Biomolecular Spectroscopy, **229**, 117912, (2020). DOI: 10.1016/j.saa.2019.117912.

- Bhumi A. Baraiya, Venu Mankad, Prafulla K. Jha, CO_2 hydrogenation to Methanol, Formic acid and Methane over Pd_5Cu_8 cluster: A First-principles Study. (To be submitted)

Chapter 5 focuses to investigate the CO oxidation mechanism over the $Cu_2O(111)$ supported Pt_4 and Pt_3X (X = Co and Au) clusters using dispersion corrected spin-polarized DFT calculations. The L-H reaction pathway considered to perform CO oxidation over considered systems. This chapter establishes the superior role of support in the stabilization of free clusters and elimination of Pt-poisoning during CO oxidation via substitutional doping.

- Bhumi A. Baraiya, Venu Mankad, Prafulla K. Jha, Determining the CO Oxidation Activity of Supported Pt_3M Clusters from Frontier Orbitals. (To be submitted)

Chapter 6 concludes and summarizes the most important findings and potential applications of the work presented in **Chapters 3-5**. This chapter also includes the future research directions and scope in the field of rational design of novel free and oxide supported heterogeneous catalysts (NCs and NAs) with improved strategy and testimonials.

References

1. J. J. Berzelius, *Ann. Chim. Phys.* **61**, 146-151, (1836).
2. R. Jin, G. Li, S. Sharma, Y. Li, X. Du, *Chem. Rev.* **121**, 567-648, (2021).
3. J. K. Nørskov, F. Studt, F. Abild-Pedersen, T. Bligaard, Fundamental Concepts in Heterogeneous Catalysis, John Wiley & Sons, Inc., (2014). DOI: 10.1002/9781118892114.
4. M. Bowker, The Basis and Application of Heterogeneous Catalysis, Oxford University Press, (1998).
5. B. Hammer, J. K. Nørskov, *Adv. Catal.* **45**, 71-129 (2000).
6. S. K. Kaiser, Z. Chen, D. F. Akl, S. Mitchell, J. Pérez-Ramírez, *Chem. Rev.* **120**, 11703-11809, (2020).
7. J. Hagen, Industrial Catalysis: A Practical Approach, Wiley-VCH, (2015).
8. G. Hutchings, M. Davidson, R. Catlow, C. Hardacre, N. Turner, P. Collier, Modern Developments in Catalysis, World Scientific Publishing Co. Pte Ltd, (2017).
9. C. M. Friend, B. Xu, *Acc. Chem. Res.* **50**, 517-521, (2017).
10. C. W. Jones, *ACS Catal.* **8**, 11908-11909, (2018).
11. Z. Li, S. Ji, Y. Liu, X. Cao, S. Tian, Y. Chen, Z. Niu, Y. Li, *Chem. Rev.* **120**, 623-682, (2020).
12. K. Yamamoto, T. Imaoka, M. Tanabe, T. Kambe, *Chem. Rev.* **120**, 1397-1437, (2020).
13. L. Zhang, M. Zhou, A. Wang, T. Zhang, *Chem. Rev.* **120**, 683-733, (2020).
14. R. Imbihl, G. Ertl, *Chem. Rev.* **95**, 697-733, (1995).
15. G. Li, R. Jin, *Acc. Chem. Res.* **46**, 1749-1758, (2013).
16. J. Zhao, R. Jin, *Nano Today* **18**, 86-102, (2018).
17. S. Yamazoe, T. Yoskamtorn, S. Takano, S. Yadnum, J. Limtrakul, T. Tsukuda, *Chem. Rec.* **16**, 2338-2348, (2016).
18. Z-J. Zhao, S. Liu, S. Zha, D. Cheng, F. Studt, G. Henkelman, J. Gong, *Nat. Rev. Mater.* **4**, 792-804, (2019).
19. R-P. Ye, J. Ding, W. Gong, M. D. Argyle, Q. Zhong, Y. Wang, C. K. Russell, Z. Xu, A. G. Russell, Q. Li, et al., *Nat. Commun.* **10**, 5698-5713, (2019).
20. J. K. Nørskov, T. Bligaard, J. Rossmeisl, C. H. Christensen, *Nat. Chem.* **1**, 37-46, (2009).
21. J. K. Nørskov, F. Abild-Pedersen, F. Studt, T. Bligaard, *Proc. Natl. Acad. Sci.* **108**, 937-943, (2011).

22. Y. Sun, Z. Xue, Q. Liu, Y. Jia, Y. Li, K. Liu, Y. Lin, M. Liu, G. Li, C-Y. Su, *Nat. Commun.* **12,** 1369-1376, (2021).
23. S. Bhattacharjee, U. V. Waghmare, S. C. Lee, *Sci. Rep.* **6**, 35916-35926, (2016).
24. B. Hammer, J. K. Nørskov, *Nature* **376**, 238-240, (1995).
25. B. Hammer, Y. Morikawa, J. K. Nørskov, *Phys. Rev. Lett.* **76**, 2141-2144, (1996).
26. M. Mavrikakis, B. Hammer, J. K. Nørskov, *Phys. Rev. Lett.* **81**, 2819-2822, (1998).
27. J. Greeley, M. Mavrikakis, *Nat. Mater.* **3**, 810-815, (2004).
28. F. Abild-Pedersen, J. Greeley, F. Studt, J. Rossmeisl, T. R. Munter, P. G. Moses, E. Skúlaso, T. Bligaard, J. K. Nørskov. *Phys. Rev. Lett.* **99**, 016105-016109, (2007).
29. B. Huang, H. Kobayashi, T. Yamamoto, T. Toriyama, S. Matsumura, Y. Nishida, K. Sato, K. Nagaoka, M. Haneda, W. Xie, et al., *Angew. Chem. Int. Ed.* **131**, 2252-2257, (2019).
30. Y-L. Lee, J. Kleis, J. Rossmeisl, Y. Shao-Horn, D. Morgan, *Energy Environ. Sci.* **4**, 3966-3970, (2011).
31. J. Suntivich, K. J. May, H. A. Gasteiger, J. B. Goodenough, Y. Shao-Horn, *Science* **334**, 1383-1385, (2011).
32. F. Studt, I. Sharafutdinov, F. Abild-Pedersen, C. F. Elkjær, J. S. Hummelshøj, S. Dahl, Ib. Chorkendorff, J. K. Nørskov, *Nat. Chem.* **6**, 320-324, (2014).
33. H. Xin, A. Vojvodic, J. Voss, J. K. Nørskov, F. Abild-Pedersen, *Phys. Rev. B* **89**, 115114-115119, (2014).
34. F. Calle-Vallejo, D. Loffreda, M. T M Koper, P. Sautet, *Nat. Chem.* **7**, 403-410, (2015).
35. F. Calle-Vallejo, J. Tymoczko, V. Colic, Q. H. Vu, M. D. Pohl, K. Morgenstern, D. Loffreda, P. Sautet, W. Schuhmann, A. S. Bandarenka, *Science* **350**, 185-189 (2015).
36. I. C. Man, H-Y. Su, F. C. Vallejo, H. A. Hansen, J. I. Martinez, N. G. Inoglu, J. Kitchin, T. F. Jaramillo, J. K. Nørskov, J. Rossmeisl, *ChemCatChem* **3**, 1159-1165 (2011).
37. X. Ma, H. Xin, *Phys. Rev. Lett.* **118**, 036101-036106, (2017).
38. R. Chattot, O. L. Bacq, V. Beermann, S. Kühl, J. Herranz, S. Henning, L. Kühn, T. Asset, L. Guétaz, G. Renou, et al., *Nat. Mater.* **17**, 827-833, (2018).
39. D. Wu, C. Dong, H. Zhan, X-W. Du, *J. Phys. Chem. Lett.* **9**, 3387-3391, (2018).
40. S. Liu, Z-J. Zhao, C. Yang, S. Zha, K. M. Neyman, F. Studt, J. Gong, *ACS Catal.* **9**, 5011-5018 (2019).
41. R. Ferrando, J. Jellinek, R. L. Johnston, *Chem. Rev.* **108**, 845-910, (2008).
42. M. Faraday, *Phil. Trans. R. Soc.* **147**, 145-181, (1857).

43. M. Gaudry, E. Cottancin, M. Pellarin, J. Lermé, L. Arnaud, J. R. Huntzinger, J. L. Vialle, M. Broyer, J. L. Rousset, M. Treilleux, et al., *Phys. Rev. B* **67**, 155409-155419, (2003).
44. R. L. Johnston, Atomic and Molecular Clusters, Taylor and Francis, (2002).
45. A. Fortunelli, G. Barcaro, Density-Functional Theory of Free and Supported Metal Nanoclusters and Nanoalloys. Metal Clusters and Nanoalloys: From Modeling to Applications, Springer, (2013).
46. X. Kang, Y. Li, M. Zhu R. Jin, *Chem. Soc. Rev.* **49**, 6443-6514, (2020).
47. N. D. Lang, W. Kohn, *Phys. Rev. B* **8**, 3541-3550, (1973).
48. W. D. Knight, K. Clemenger, W. A. de Heer, W. A. Saunders, M. Y. Chou, M. L. Cohen, *Phys. Rev. Lett.* **52**, 2141-2143, (1984).
49. Z. Penzar, W. Ekardt, *Z. Phys. D* **17**, 69-72, (1990).
50. B. A. Baraiya, H. Tanna, V. Mankad, P. K. Jha, *J. Phys. Chem. A* **125**, 5256-5272, (2021).
51. A. M. Molenbroek, J. K. Nørskov, B. S. Clausen, *J. Phys. Chem. B* **105**, 5450-5458, (2001).
52. S. Zhou, B. Varughese, B. Eichhorn, G. Jackson K. McIlwrath, *Angew. Chem. Int. Ed.* **44**, 4539-4543, (2005).
53. A. M. Molenbroek, S. Haukka, B. S. Clausen, *J. Phys. Chem. B* **102**, 10680-10689, (1998).
54. M. M. Maye, Y. Lou C-J. Zhong, *Langmuir* **16**, 7520-7523, (2000).
55. B. Coq, F. Figueras, *J. Mol. Catal. A: Chem.* **173**, 117-134, (2001).
56. J. C. Fuggle, F. U. Hillebrecht, R. Zeller, Z. Zołnierek, P. A. Bennett, C. Freiburg, *Phys. Rev. B* **27**, 2145-2178, (1983).
57. A. M. Venezia, L. F. Liotta, G. Deganello, Z. Schay, L. Guczi, *J. Catal.* **182**, 449-455, (1999).
58. B. Coq, A. Goursot, T. Tazi, F. Figuéras, D. R. Salahub, *J. Am. Chem. Soc.* **113**, 1485-1492, (1991).
59. S. Ma, M. Sadakiyo, M. Heima, R. Luo, R. T. Haasch, J. I. Gold, M. Yamauchi, P. J. A. Kenis, *J. Am. Chem. Soc.* **139**, 47-50, (2017).
60. X. Jiang, X. Nie, X. Wang, H. Wang, N. Koizumi, Y. Chen, X. Guo, C. Song, *J. Catal.* **369**, 21-32, (2019).
61. L. Liu, A. Corma, *Chem. Rev.* **118**, 4981-5079, (2018).
62. H-J. Freund, *Sur. Sci.* **500**, 271-299, (2002).
63. M. Haruta, T. Kobayashi, H. Sano, N. Yamada, *Chem. Lett.* **16**, 405-408, (1987).

64. J. C. Fierro-Gonzalez, B. C. Gates, *Chem. Soc. Rev.* **37**, 2127-2134, (2008).
65. J. K. Edwards, B. Solsona, E. Ntainjua, A. F. Carley, A. A. Herzing, C. J. Kiely, G. J. Hutchings, *Science* **323**, 1037-1041, (2009).
66. G. Kyriakou, S. K. Beaumont, S. M. Humphrey, C. Antonetti, R. M. Lambert, *ChemCatChem* **2**, 1444-1449, (2010).
67. M. Chen, D. W. Goodman, *Chem. Soc. Rev.* **37**, 1860-1870, (2008).
68. M. Valden, X. Lai, D. W. Goodman, *Science* **281**, 1647-1650, (1998).
69. M. Haruta, N. Yamada, T. Kobayashi, S. Iijima, *J. Catal.* **115**, 301-309, (1989).
70. M. M. Schubert, S. Hackenberg, A. C. van Veen, M. Muhler, V. Plzak, R. J. Behm, *J. Catal.* **197**, 113-122, (2001).
71. S. Carrettin, P. Concepción, A. Corma, J. M. L. Nieto, V. F. Puntes, *Angew. Chem. Int. Ed.* **43**, 2538-2540, (2004).
72. N. Weiher, E. Bus, L. Delannoy, C. Louis, D. Ramaker, J. T. Miller, J. A. van Bokhoven, *J. Catal.* **240**, 100-107, (2006).
73. A. Hinz, P-O. Larsson, B. Skårman, A. Andersson, *Appl. Catal. B* **34**, 161-178, (2001).
74. M. Chandra, Q. Xu, *J. Power Sources* **168**, 135-142, (2007).
75. A. Wolf, A. J. Jess, C. K. Kern, *Chem. Eng. Technol.* **39**, 1040-1048, (2016).
76. X. Jiang, X. Nie, X. Guo, C. Song, J. G. Chen, *Chem. Rev.* **120**, 7984-8034, (2020).
77. Y. Hartadi, D. Widmann, R. J. Behm, *J. Catal.* **333**, 238–250, (2016).
78. S. Rai, M. Ehara, U. D. Priyakumar, *Phys. Chem. Chem. Phys.* **17**, 24275-24281, (2015).
79. S. Navarro-Jaén, M. Virginie, J. Bonin, M. Robert, R. Wojcieszak, A. Y. Khodakov, *Nat. Rev. Chem.* **5**, 564-579, (2021).
80. Methanol Market Size, Analysis & Trends - Industry Report, 2019-2026, Polaris Market Research Report, (2019).
81. C. Hepburn, E. Adlen, J. Beddington, E. A. Carter, S. Fuss, N. M. Dowell, J. C. Minx, P. Smith, C. K. Williams, *Nature* **575**, 87-97, (2019).
82. Y. Liu, L. Guo, *J. Chem. Phys.* **152**, 100901-100912, (2020).
83. B. A. Baraiya, V. Mankad, P. K. Jha, *Spectrochim. Acta A* **229**, 117912-117920, (2020).